Case Studies in Construction Materials 22 (2025) e04103

Contents lists available at ScienceDirect

Case Studies in Construction Materials

journal homepage: www.elsevier.com/locate/cscm

Optimising thermo-mechanical treatments of residual rice husk ash for cement blending

Ayman Almutlaqah [a,b], Riccardo Maddalena [a], Sivakumar Kulasegaram [a,*]

[a] School of Engineering, Cardiff University, Cardiff, UK
[b] Civil Engineering Department, College of Engineering, Najran University, Najran, Saudi Arabia

ARTICLE INFO

Keywords:
Rice husk ash (RHA)
Microstructure
Thermal treatment
Grinding process
Mechanical activation
Cement hydration
Pozzolanic activity

ABSTRACT

Rice husk ash (RHA) is commonly considered a promising cement replacement in concrete; however, RHA obtained through uncontrolled combustion often exhibits limited pozzolanic activity due to excess unburnt carbon and a porous structure. This study investigates the effect of microstructure on the burning process for enhancing RHA properties and reducing cement content in the binder. Coarse RHA and finely ground RHA were subjected to burning at various temperatures and durations, with Particle size distribution (PSD), Scanning electron microscopy (SEM), Loss of ignition (LOI), X-ray diffraction (XRD) and fluorescence (XRF) used to investigate their properties. The pozzolanic activity index and heat of hydration were examined in mortars incorporating RHA as a cement replacement. The results demonstrated that the microstructure of RHA had a marginal effect on silica properties during the burning process, as confirmed by XRD analysis of the materials at temperatures below 800 °C. Nevertheless, noticeable variations were observed in PSD, SEM, LOI, XRF, heat of hydration, and pozzolanic activity, indicating that burning coarse RHA had more beneficial effect on combustion efficiency compared to burning finely ground RHA. This highlights the importance of an effective combustion strategy to transform residual RHA into a potent supplementary cementitious material (SCM).

1. Introduction

Rice husk (RH) is an agricultural by-product of the milling of rice [1,2]. For every tonne of rice produced, approximately 0.20 tonnes of RH are generated [1,3,4]. The global production of rice in 2022 has been estimated at 515.05 million tonnes [5]. This suggests that an enormous quantity of RH is produced annually, but the majority of this RH is underutilised, discarded in landfills, or burned in open fields, which has long-term environmental implications [2,6]. The common practice to mitigate this issue is to reuse RH as fuel for industrial heat production [6–8]. When RH is burned as fuel, a by-product called rice husk ash (RHA) is produced at a rate of 20–25 % of the weight of RH [7,9]. Although RHA has many commercial applications, it is usually discarded in landfills because of inadequate guidelines and specifications for its use in developing countries [6]. This disposal can have adverse environmental consequences, such as soil and water pollution, ultimately affecting human health [6].

The availability and favourable chemical composition of RHA make it a viable supplementary material in cement composite applications [6,10]. The composition of RHA varies depending on the rice source, soil chemistry, and geographic location [6,8,11]. The nature of silica formation can be different in dark- versus light-coloured ash depending on the presence of unburnt carbon impurities

* Corresponding author.
E-mail address: KulasegaramS@cardiff.ac.uk (S. Kulasegaram).

https://doi.org/10.1016/j.cscm.2024.e04103
Received 11 June 2024; Received in revised form 4 December 2024; Accepted 9 December 2024
Available online 9 December 2024

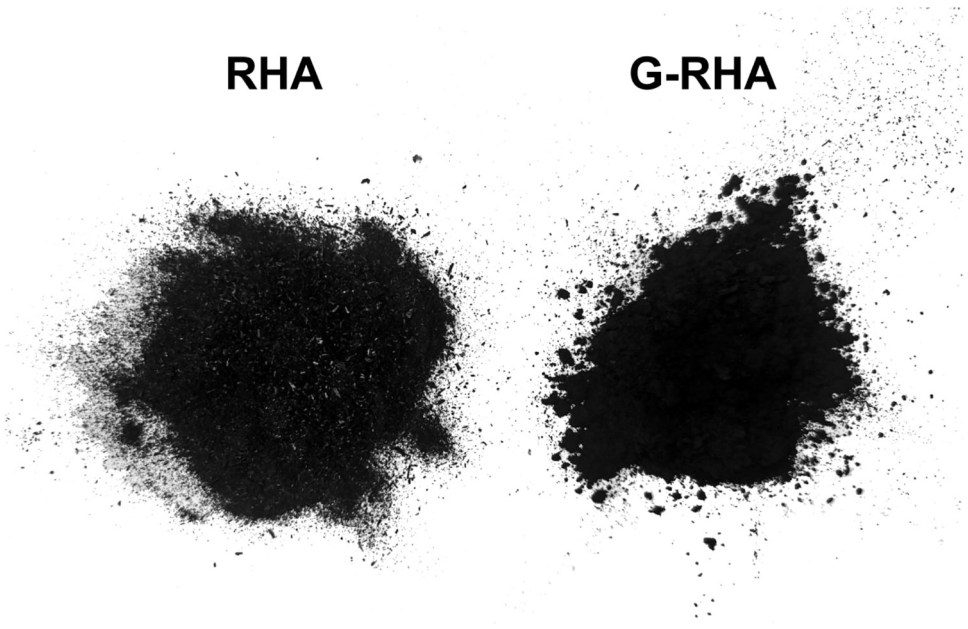

Fig. 1. The raw RHA received for this study and ground RHA (G-RHA).

[11], which in turn depends on the combustion equipment and the conditions of producing the RHA [12,13]. The RHA produced by uncontrolled combustion is unlike the one produced by controlled combustion. Uncontrolled combustion such as open field burning or open heap burning is a conventional process used for disposing of RH in various areas of the world and close to the rice milling factories [6,7,10,13]. The RHA produced by uncontrolled combustion tends to be black in colour because of unburnt carbon trapped beneath the molten surface of the ash [3,8,13,14]. This phenomenon occurs when potassium oxide decomposes during the combustion of RH, hindering the heterogeneous dispersion of heat and airflow [11,15]. In other words, during the conversion of RH to ash, uncontrolled combustion, resulting from its heterogeneous dispersion of oxygen, causes the rapid decomposition of potassium oxide into molten substances on the surface. This molten layer restricts the carbon from oxidising and accelerates the crystallization of SiO_2 [11,15]. Under these conditions, RHA has low pozzolanic activity. The excess residue carbon contents on the ash also lead to more water absorption in the concrete. Therefore, adopting RHA generated under uncontrolled burning conditions as a cement replacement material is not feasible unless further treatments are employed [3,13,16,17].

One method to increase the effectiveness of RHA received from uncontrolled combustion is thermal treatment before blending with cement. Research suggests that this reduces the residual unburnt carbon and produces more effective RHA [8]. Typically, with rising temperatures, the crystalline structure might be destructed, leading to create of amorphous silica; however, this depends on appropriate temperature and duration of the combustion. If RHA subjected to higher temperature and extended period of combustion, the amorphous silica can be transformed back to its original crystalline state [18–22]. Thermal treatment of black RHA from uncontrolled combustion has been conducted in many studies [8,13,14,23].

Another typical approach to enhancing the pozzolanic activity of RHA is to break down the cellular microstructure of the particles and decrease their size [6,7,10]. Mehta [24] observed that the pozzolanic activity of RHA depends mainly on the internal surface area of the particles. Xu [25] confirmed that decreasing the particle size of RHA affects its pozzolanic activity and showed that the pozzolanic reactivity of RHA increases as the ash becomes finer, with no corresponding effects on the proportion of crystalline and amorphous silica in the ash.

Although the available literature has established the relationship between the heat treatment and grinding of RHA and its pozzolanic activity, it is not clear how the microstructure of RHA affects the burning process to enhance its reactivity most effectively. Therefore, there remains a need to study the effect of burning both coarse and fine RHA. This study aims to provide recommendations and, outline a feasible insight for proposing RHA from uncontrolled combustion as a Portland cement replacement material. This can benefit not just in the proper disposal of the residual RHA, but also in reducing the cost of the concrete.

RHA obtained from an industrial source was subjected to various trial treatments, namely, 1) grinding prior to thermal treatment at various temperatures and for various durations and 2) thermal treatment at various temperatures and for various durations followed by grinding.

Particle size distribution (PSD), Scanning electron microscopy (SEM), Loss on ignition (LOI), X-ray diffraction (XRD) and fluorescence (XRF) were used to investigate the properties of the supplied and treated RHA. The pozzolanic activity and heats of hydration of mortars made with treated RHA as a partial cement replacement were examined.

Table 1
Chemical composition and physical properties of the Portland cement (OPC, type I 52.5 MPa) and RHA used.

Composition	Cement	RHA
SiO_2 (%)	19.69	79.86
Al_2O_3 (%)	4.32	-
Fe_2O_3 (%)	2.85	0.15
CaO (%)	63.04	1.11
K_2O (%)	0.74	3.23
Na_2O (%)	0.16	-
MgO (%)	2.17	-
SO_3 (%)	3.12	0.15
TiO_2 (%)	0.33	-
Specific gravity	3.15	2.03
Fineness (m^2/kg)	384	-
Initial Setting Time (mins)	158	-
Loss on ignition (%)	3.03	13.49

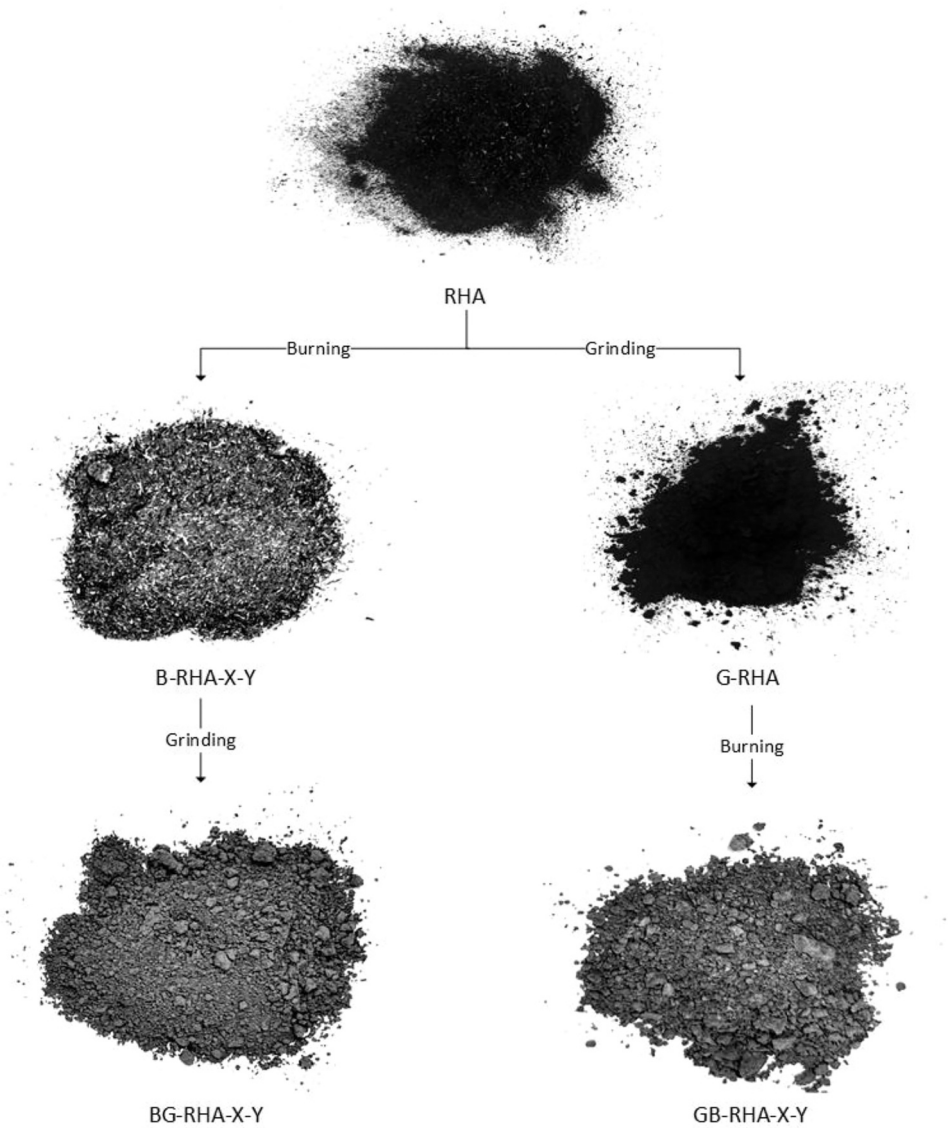

Fig. 2. Thermo-mechanical treatment flowchart of RHA (G and B indicate respectively grinding and/or burning processes. X indicates the burning temperature in °C and Y indicates the burning duration in hours).

Table 2
Mix proportions by weight of the mortar for the strength activity and heat of hydration tests. water/binder (w/b) ratio; aggregate/binder (a/b) ratio; Standard deviation of the flow table test results (St. Dv).

Symbol		w/b	a/b	Flow %	St. Dv.
Control		0.48	2.75	63.75	0.25
As received RHA		0.71	2.75	66.25	0.30
B-RHA-X-Y	B-RHA−400–3	0.68	2.75	59.25	0.15
	B-RHA−400–6	0.68		64.00	0.45
	B-RHA−500–3	0.68		59.00	0.45
	B-RHA−500–6	0.68		63.25	0.17
	B-RHA−600–3	0.68		68.50	0.44
	B-RHA−600–6	0.67		65.00	0.24
	B-RHA−700–3	0.65		58.75	0.10
	B-RHA−700–6	0.65		66.75	0.28
	B-RHA−800–3	0.65		59.00	0.36
	B-RHA−800–6	0.65		68.50	0.31
G-RHA		0.50	2.75	59.00	0.41
GB-RHA-X-Y	GB-RHA−400–3	0.50	2.75	62.00	0.16
	GB-RHA−400–6			63.50	0.10
	GB-RHA−500–3			58.5	0.19
	GB-RHA−500–6			58.00	0.46
	GB-RHA−600–3			59.25	0.43
	GB-RHA−600–6			61.00	0.20
	GB-RHA−700–3			60.00	0.16
	GB-RHA−700–6			61.75	0.17
	GB-RHA−800–3			67.50	0.29
	GB-RHA−800–6			61.25	0.48
BG-RHA-X-Y	BG-RHA−400–3	0.50	2.75	59.75	0.21
	BG-RHA−400–6			58.75	0.25
	BG-RHA−500–3			59.00	0.12
	BG-RHA−500–6			63.00	0.12
	BG-RHA−600–3			62.25	0.21
	BG-RHA−600–6			58.75	0.30
	BG-RHA−700–3			61.88	0.63
	BG-RHA−700–6			58.75	0.48
	BG-RHA−800–3			63.00	0.12
	BG-RHA−800–6			62.50	0.19

2. Materials and experimental methods

2.1. Materials

Mortar specimens were prepared by mixing Ordinary Portland cement, RHA, standard river sand and water at different ratios. Ordinary Portland cement (OPC, type I 52.5 MPa) conforming to the EN-197–1 standard was used [26]. The fine aggregate used was a natural river sand with a maximum size of 1.18 mm. The RHA used in this study was sourced from Supsuvan Industry Co., Ltd., Thailand, where RH underwent uncontrolled combustion at approximately 475 °C between 30 min and 1 hour. This product tends to have a dark colour and irregularly shaped particles (Fig. 1). The chemical compositions of the OPC and RHA products obtained through XRF are shown in Table 1.

2.2. Sample preparation and testing program

The black colour appearance of the RHA is caused by uncontrolled burning during the thermal conversion of RH to RHA, leading to a non-uniform distribution of oxygen, a high rate of crystallisation, and poor pozzolanic reaction [11,13]. Additionally, as shown in Fig. 1, the particles of RHA are porous and cellular in nature, with unburnt carbon impurities in the ash, which can cause water demand issues [3,9,16,17]. Under these conditions, using RHA as a partial substitution for cement in concrete is not ideal [11,17]. Della et al. [8] reported that the structure of RHA is not only affected by heat treatment; it is also possible to convert black RHA into valuable raw materials after heat treatment and grinding. The black coarse RHA received was treated using thermal treatment (burning, B) in a furnace, mechanical grinding (G) and a combination of the following mechanical and thermal treatments either burning then grinding and vice versa, as explained below and in Fig. 2:

1. Burning (B) at various temperatures and durations: the burnt samples denoted by B-RHA-X-Y. The RHA was placed in a furnace and heated at a rate of 10 °C/min to maximum temperatures of 400, 500, 600, 700, and 800 °C for either 3 or 6 h. The samples were then left in the furnace to cool down to room temperature.
2. Grinding process (G): ground samples are denoted as G-RHA. Grinding was performed using a vibratory disc mill for 5 min/100 g to allow the particles to break down and decrease the overall particle size (see Fig. 1).

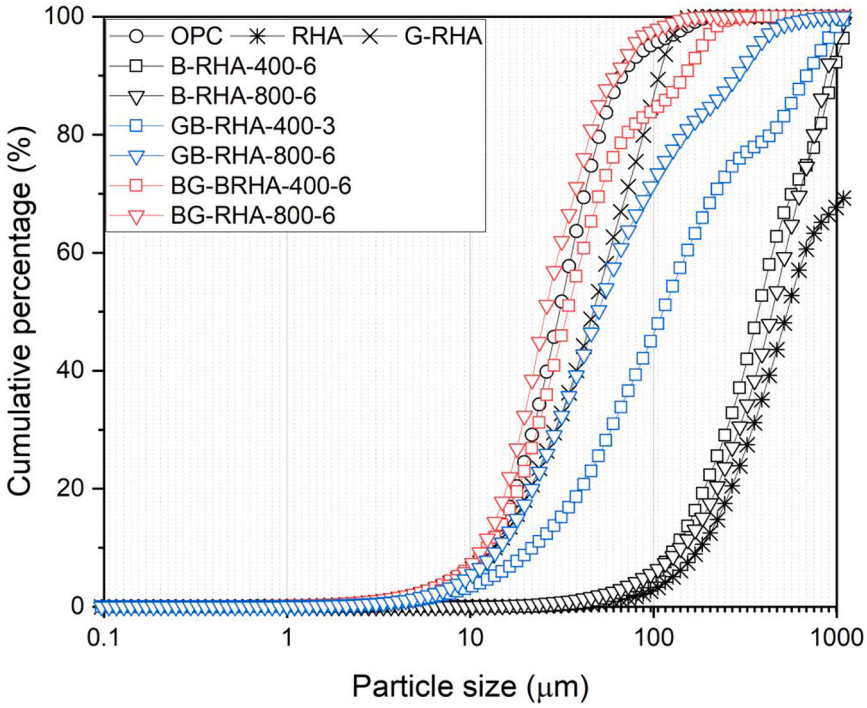

Fig. 3. Particle size distribution of the materials of Ordinary Portland cement (OPC), as received rice husk ash (RHA), ground RHA (G-RHA), burnt ground RHA (GB-RHA-X-Y), burnt RHA followed by grinding (BG-RHA-X-Y). The 3-digit number (X) indicate the temperature (in °C) of the thermal treatment, and the final digit (Y) indicates the duration in hours.

3. Grinding (G) before burning (B): RHA samples was ground into a powder and then burned at various temperatures and durations. These samples are denoted as GB-RHA-X-Y.
4. Burning (B) before grinding (G): RHA samples was burned and then ground to reduce its particle size. These samples are denoted as BG-RHA-X-Y, where X denotes the temperature in °C and Y denotes the duration in hours.

These different treatments were designed for the purpose of examining RHA's microstructure, assessing its combustion efficiency in carbon removal, investigating its impact on the silica phase within the ash, and evaluating its compatibility with binders in mortar.

The particle size distribution of the materials was determined by laser diffraction technology using a Beckman Coulter LS 13 320 XR particle size analyser. The weight of cement used to produce the mortar mix was 666.6 Kg/m^3 replaced with 20 % RHA, and the weight of the aggregate sand was 1833.3 Kg/m^3 [27]. The mix compositions of the mortars are listed in Table 2. The control mortars were mixed at a water/binder (w/b) ratio of 0.48 and an aggregate/binder (a/b) ratio of 2.75. The w/b ratios of the mortars containing RHA were modified to achieve a flow within ± 5 % of that of the control mortar, as measured by the flow table test [27].

2.2.1. Loss of ignition weight and scanning electron microscopy

Loss of ignition weight was tested on the coarse and finely ground RHA as per ASTM D734–2021 [28]. Scanning electron microscopy (SEM) using energy dispersive spectroscopy (EDS) was performed on the coarse and finely ground RHA before and after thermal treatment at selected temperature (400 °C) using a Carl Zeiss Sigma HD Field Emission Gun SEM. Secondary electron images (SEIs) were captured at a 15-mm working distance, 10 kV, a final aperture diameter of 60 μm, and a beam current of 1.5 nA.

2.2.2. X-ray diffraction and fluorescence

XRD was used to assess the crystallinity degree of the silica in the ash. Scans were carried out with a Philips PW1710 Automated Powder Diffractometer using Cu Kα radiation at 35 kV and 40 mA with a range of 10–60° 2θ at a scan speed rate of 0.04° 2θ/s. Phase identification was done using the Philips PC Identify software, and the peak areas were used to perform a semi-quantitative analysis and to calculate the percentage of each phase present. The effect of the sequential order of thermal treatment and grinding processes on the chemical composition of RHA was analysed using XRF at selected temperatures of 400 °C and 800 °C.

2.2.3. Pozzolanic activity

The strength activity index (SAI) defined by ASTM C311- 2022 [27] was used to assess the pozzolanic activity of the RHA and its suitability for partial substitution of cement. A control mortar with no RHA replacement served as a reference for SAI measurement. The cement mortar mix was poured into a cubic steel mould (50 mm) and manually compacted by tamper. Following a 24-hour curing

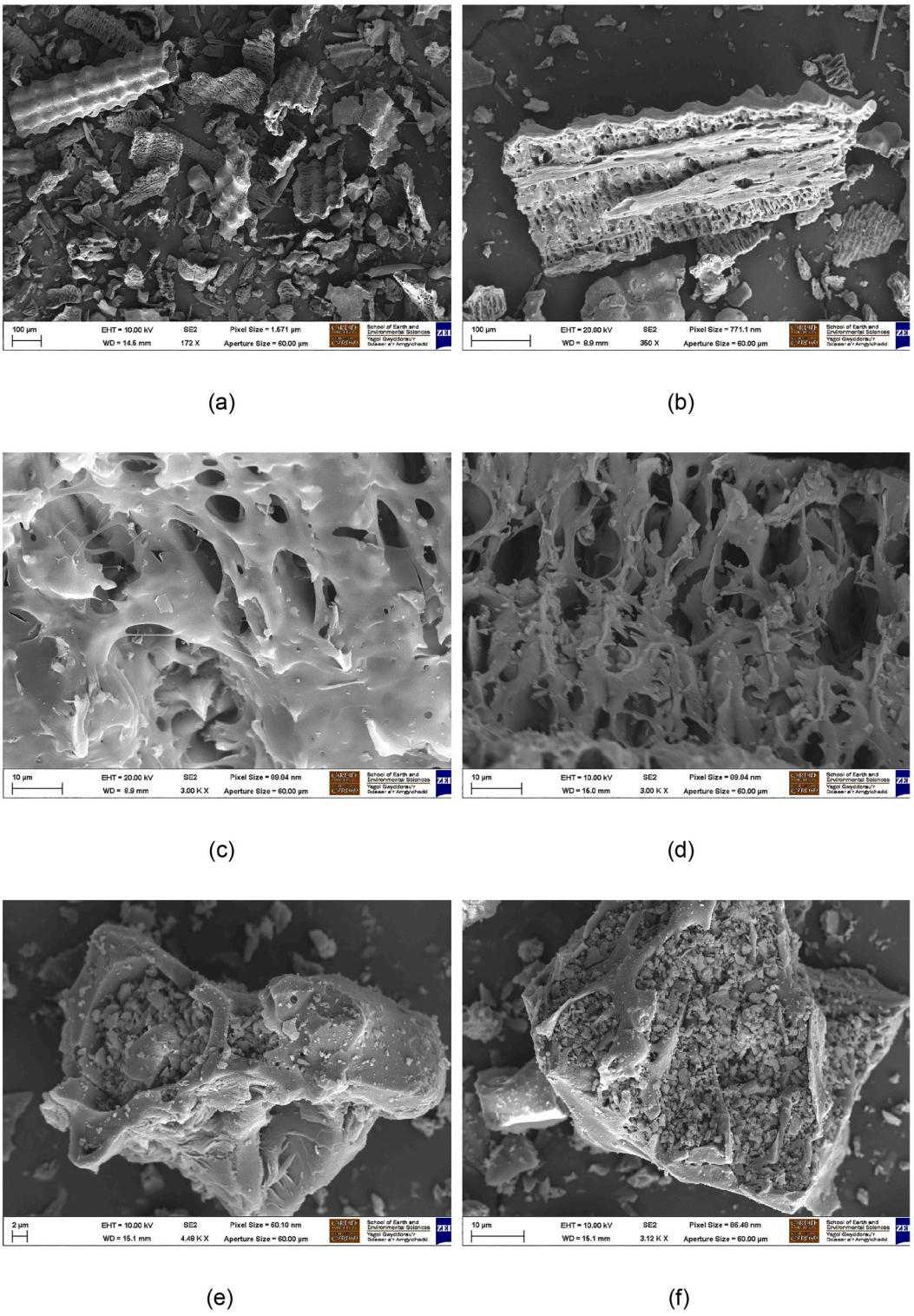

Fig. 4. SEM of selected RHA: (a) overview of the particles, (b) particles layers, (c) interlayer structure of received RHA, (d) interlayer structure of burnt RHA (B-RHA-400–6), (e) and (f) porous structure of RHA subjected to burning following by grinding (BG-RHA-400–6).

Table 3
XRF results of selected treated RHA samples.

Symbol	SiO_2 (%)	K_2O (%)	CaO (%)	Other%
RHA	79.86	3.23	1.11	0.30
B-RHA−400–6	86.04	3.05	1.11	0.29
B-RHA−800–6	86.47	3.10	1.19	0.18
G-RHA	70.48	2.50	1.02	0.27
GB-RHA−400–6	83.92	2.53	1.21	0.43
GB-RHA−800–6	78.40	2.44	1.04	0.35
BG-RHA−400–6	79.64	2.73	1.60	0.56
BG-RHA−800–6	77.71	2.63	1.28	0.51

Table 4
Loss of ignition (LOI %) of received coarse and ground RHA subjected to different thermal treatments.

Sample	Burning temperature (°C)	Burning duration (h)	Loss on ignition (LOI %)	St. Dv.
Coarse RHA	As received from the supplier		13.49	0.240
	400	3	3.30	0.079
		6	3.11	0.009
	500	3	2.53	0.151
		6	2.43	0.042
	600	3	1.84	0.086
		6	1.78	0.103
	700	3	1.57	0.151
		6	1.50	0.282
	800	3	1.46	0.081
		6	1.05	0.147
Ground RHA	400	3	3.60	0.130
		6	3.30	0.033
	500	3	3.10	0.201
		6	3.10	0.129
	600	3	2.36	0.241
		6	2.08	0.031
	700	3	1.95	0.302
		6	1.64	0.134
	800	3	1.52	0.194
		6	1.25	0.194

period at 20 C, the samples were demoulded and placed in a saturated lime water tank for additional curing to prescribed ages. Compressive strength test was then carried out on each specimen at 7 and 28 days [27].

2.2.4. Heat of hydration

The effects of the studied treatments of the received RHA on its hydration in the test mortars were assessed using an isothermal calorimeter with eight channels (Calmetrix, I-Cal 8000 HPC) [29] at a temperature of 20 °C. The large sample size, surpassing that in previous studies [13,30], allowed for accurate monitoring of the hydration heat output in the test mortars, ensuring high precision in the results. The heat measurement readings were recorded every minute over a time span of 100 h. The heat generation rates of the samples were subsequently calculated based on their mix proportions.

3. Results

3.1. Characterisation of RHA as received and treated

3.1.1. Microstructure, elemental analysis and chemical composition

The SEM image in Fig. 4.a shows the external and internal surfaces of the RHA. The image Fig. 4.b shows interlayers containing crisscrossed meshes of chips. The chips are organised in a honeycombed arrangement consisting of many holes (Fig. 4.c). More pores can be observed after burning of the RHA (Fig. 4.d). This is attributable to the thermal decomposition of the molten layer and organic impurities in the raw RHA verified by LOI% (Table 4), which leaves pores in the structure [13,31]. In contrast, RHA particles appear to be more rounded after grinding (Fig. 5). In terms of the impact of the preference order between burning and grinding on the microstructure of RHA (Fig. 4.e, Fig. 4.f, Fig. 5.d, Fig. 5.e), it was observed that the RHA subjected to thermal treatment before grinding (BG-RHA-400–6) left more pores in structure, leading to increased fineness (see Fig. 3) compared to the RHA which underwent grinding before thermal treatment (GB-RHA-400–6). This is because grinding followed by burning results in lower decomposition of impurities, as verified by LOI results, due to the formation of surface melting.

This is verified by the XRF analysis shown in Table 3. The rapid decomposition of potassium oxide (K_2O) in RHA subjected to grinding before thermal treatment resulted in a lower fraction of the K_2O compared to RHA that underwent thermal treatment before

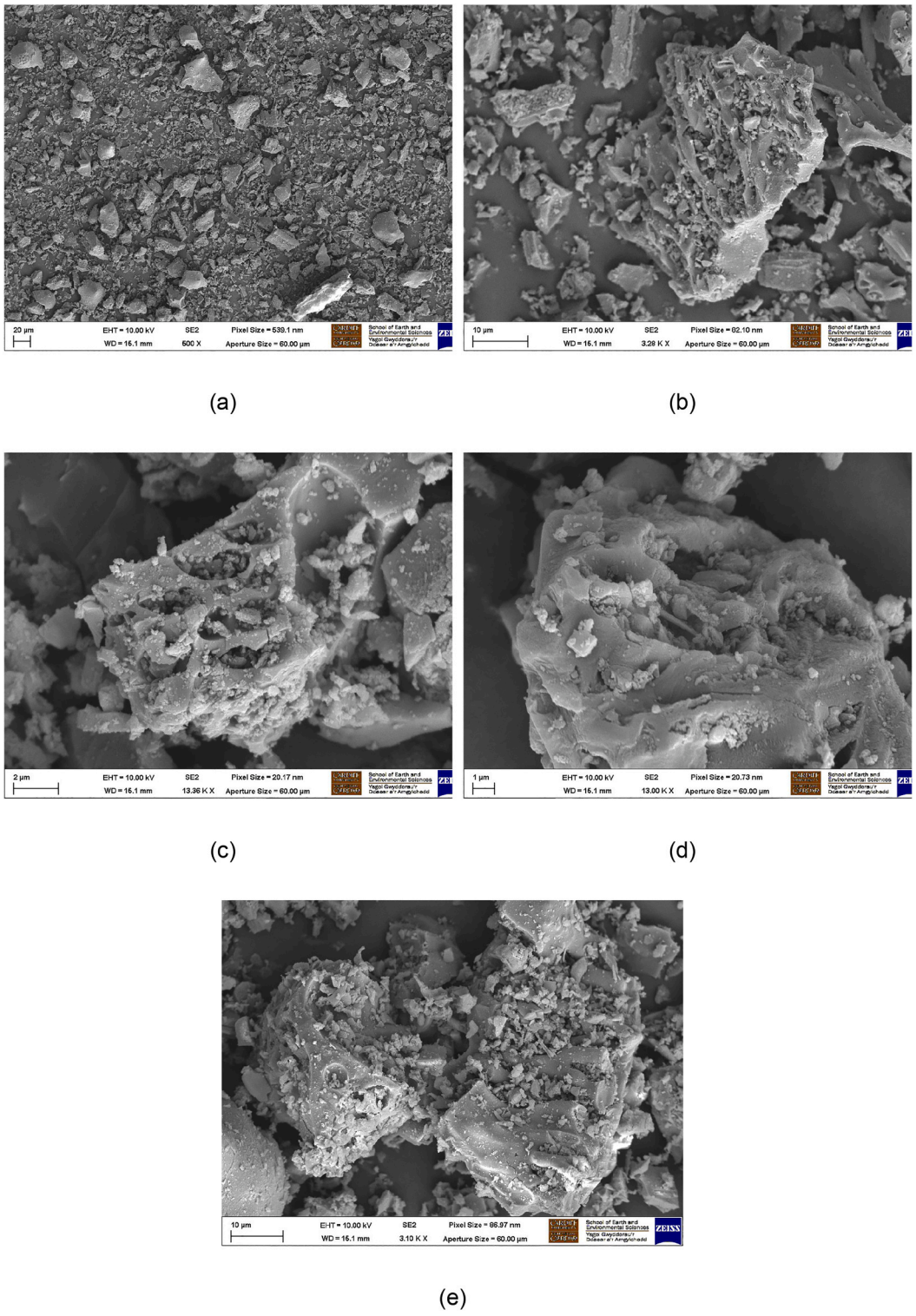

Fig. 5. SEM of selected ground RHA (G-RHA): (a) overview of the particles, (b) and (c) porous structure of G-RHA, (d) and (e) porous structure of ground RHA followed by burning (GB-RHA-400–6).

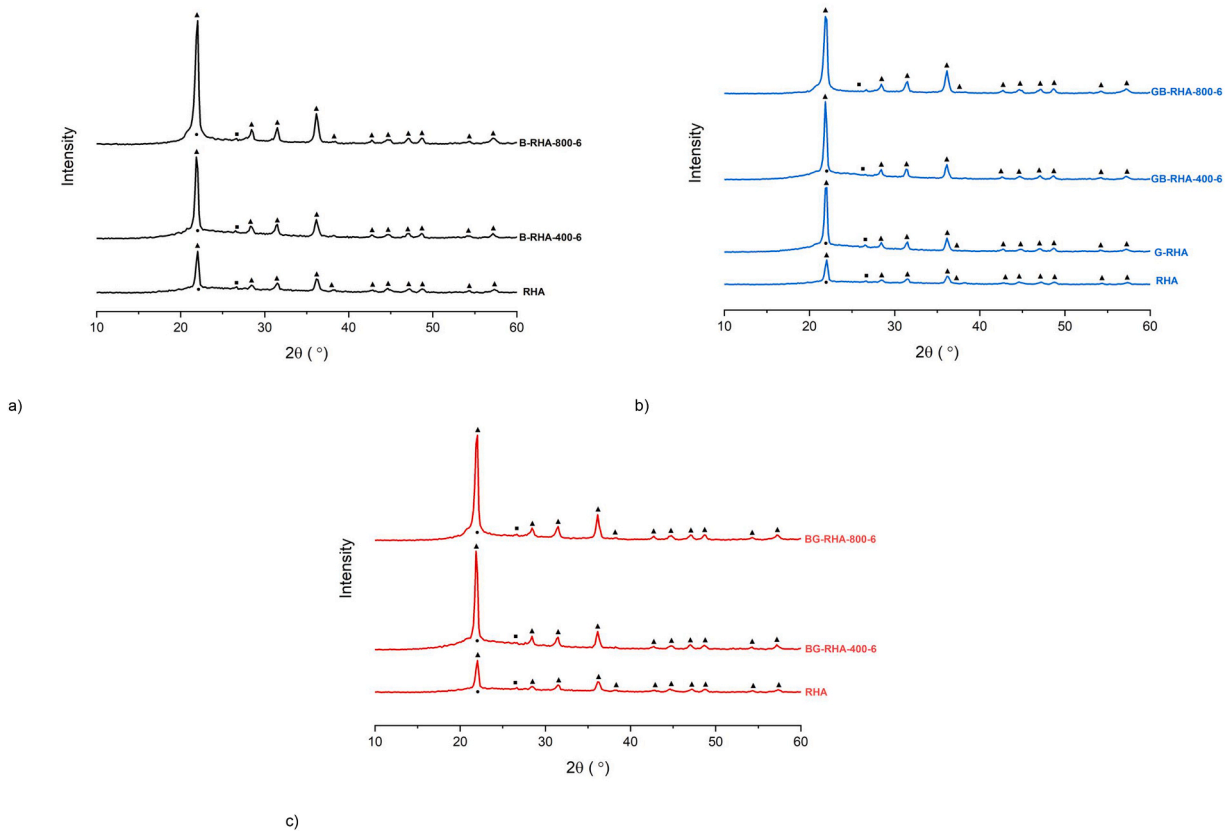

Fig. 6. XRD pattern of selected RHA as supplied and treated for detailed view, a) received RHA and burnt RHA (B-RHA), b) ground RHA (G-RHA) and burnt ground RHA (GB-RHA-X-Y), c) burnt RHA followed by grinding (BG-RHA-X-Y). (▲ = Cristobalite; ■ = Quartz; ● = Amorphous material).

grinding. For example, in the case of RHA that was burned followed by grinding (BG-RHA-400–6), the K_2O was 2.73 %. In contrast, when RHA was ground before burning (GB-RHA-400–6), the K_2O was slightly lower at 2.53 % suggesting a higher loss of potassium oxide from the original material. This confirms that the burning process of the ground RHA results in increased decomposition of the K_2O, consequently making it more challenging for organic impurities to decompose.

3.1.2. XRD analysis

The X-ray diffraction (XRD) pattern of the received RHA is shown in Fig. 6. The pattern indicates the presence of amorphous silica along with some crystalline silica (quartz and cristobalite) in RHA. However, the crystallisation rate tends to be high [11,23], which can result in poor pozzolanic activity [3,13].

The XRD pattern of the treated RHA is presented in Fig. 6. Semi-quantitative analysis was performed to determine the percentage of each phase in the samples by assessing the peak areas of the major peaks for each phase in each sample. Diffractograms presenting a significant background signal suggested the presence of amorphous material, possibly corresponding to amorphous silica, based on the sample chemistry. A pronounced amorphous-like hump in the region of 20–25° 2θ indicated the development of amorphous silica phase. Higher burning temperatures caused the peaks to become sharper, indicating that the crystallite size increased with increasing temperature. The crystalline phase formation is intensified when the K_2O in RHA decomposes to molten substances [11,15]. The results are shown in Table 5.

The findings indicate that the crystallisation of silica phases was more pronounced at 800 °C, particularly for burnt ground RHA (GB-RHA). Overall, the effect of the proposed thermal treatment of RHA on its silica nature was minimal when the temperature was below 800 °C. Similar observations have been reported in previous study [32], with no significant differences being observed in the XRD patterns at temperatures below 800 °C. In addition, the findings indicate that the grinding process had a minimal effect on XRD analysis outcomes, consistent with [25].

3.2. Influence of RHA treatments on binder reactivity in mortar

3.2.1. Hydration kinetic

The isothermal calorimetry findings (Fig. 7 and Fig. 8) show that incorporating the received RHA as a binder replacement for cement resulted in the formation of different hydrated products. These, in turn, influence the stages of hydration, including the

Table 5
Semi-quantitative analysis of XRD patterns of RHA as supplied and treated.

Sample		Amorphous material %	Cristobalite %	Quartz %
Original RHA		60	38	2
B-RHA-X-Y	B-RHA−400–3	64	34	2
	B-RHA−400–6	61	37	2
	B-RHA−500–3	59	38	1
	B-RHA−500–6	58	40	2
	B-RHA−600–3	61	38	1
	B-RHA−600–6	59	39	2
	B-RHA−700–3	56	43	1
	B-RHA−700–6	55	44	1
	B-RHA−800–3	45	55	-
	B-RHA−800–6	31	68	1
G-RHA		60	37	3
GB-RHA-X-Y	GB-RHA−400–3	59	38	3
	GB-RHA−400–6	64	36	2
	GB-RHA−500–3	66	33	1
	GB-RHA−500–6	55	39	6
	GB-RHA−600–3	59	39	2
	GB-RHA−600–6	57	42	1
	GB-RHA−700–3	56	43	1
	GB-RHA−700–6	52	47	1
	GB-RHA−800–3	23	74	3
	GB-RHA−800–6	-	97	3
BG-RHA-X-Y	BG-RHA−400–3	61	37	2
	BG-RHA−400–6	62	37	1
	BG-RHA−500–3	60	37	3
	BG-RHA−500–6	61	36	3
	BG-RHA−600–3	55	44	1
	BG-RHA−600–6	57	41	2
	BG-RHA−700–3	56	43	1
	BG-RHA−700–6	54	44	2
	BG-RHA−800–3	45	54	1
	BG-RHA−800–6	36	63	1

induction period, acceleration period, deceleration period, and diffusion period (Fig. 7), which can also impact the cumulative heat output (Fig. 8). Using RHA in mortar as a partial cement replacement delayed the hydration process compared to that of the reference mortar. RHA influences cement hydration through three primary mechanisms: the pozzolanic effect, the dilution effect, and residual carbon effect [33–35]. The high silica content in RHA can contribute to decreasing the Ca/Si ratio and forming additional C-S-H products, which in turn enhances the hydration reaction [34]. However, the porous structure of RHA affects its pozzolanic reaction with cement by absorbing water. Some free water is absorbed by the pores of RHA particles during mixing, which can lower the material's w/b ratio [33,34]. As a result, the dilution effects of RHA particles in decreasing early-age hydration can be significant. Furthermore, the high carbon content and residual carbon of RHA can adversely affect cement hydration, delaying the hydration peak [35].

It is seen that the main peak in the acceleration period is erratic showing two peaks due to different reactivity of different cement minerals. More C_3S phase hydrated in the first hours, as indicated in the first hydration peak, resulting in greater heat release. Then the heat of hydration rate starts to decrease as the hydration of C_3S is impeded. In the interval between the initial and subsequent peak, the hydration of the less reactive C_2S phase starts to take place, resulting in an increased rate of heat emission. Generally, the total heat generated during the second peak is higher than that during the first peak, because the overall heat generated by the combined of hydration of C_3S and C_2S is higher than that generated merely by C_3S [36–38]. The height of the second peak was observed to slightly increase when treated RHA was used (Fig. 7.b and Fig. 7.c) with cement in the mortar, due to the nature of pozzolanic products. The first peak is related to the rapid hydration reaction between cement and water, whereas the second peak is related to the pozzolanic reaction of RHA with calcium hydroxide resulting in the production of C-S-H phases [33–35].

The heat flow of control samples reached its peak at about 14 h. For the samples containing RHA, it is found that the heat flow reached its maximum at much later stage. Burning RHA to remove residual carbon slightly contributed to the development of hydration kinetics. This is because residual carbon in the ash absorbs more water and retards the hydration of the mortar [3,13,35]. The kinetic hydration of the burnt ash at 400 °C was more pronounced than that at 800 °C because of the presence of amorphous silica. Despite the high silica content in RHA, the maximum heat flow of the samples containing burnt RHA is still lower than that of the control sample. Grinding RHA finely to break down its cellular structure has a tendency to improve the hydration kinetics due to filler effects [17,25]. Decreasing the particle size and disrupting the cellular structure enhances the homogeneity of the material and increases its fineness. This contributes to an increase in the C-S-H content and enhances the hydration reaction since finer particles provide more nucleation sites, leading to higher reactivity [17,25]. Therefore, G-RHA exhibited enhanced hydration kinetics. The effects of the difference between thermal treatment and grinding can take place during the hydration process. Burning the RHA prior to grinding resulted in slightly more pronounced reactivity because its effectiveness in removing carbon impurities (see the LOI values in

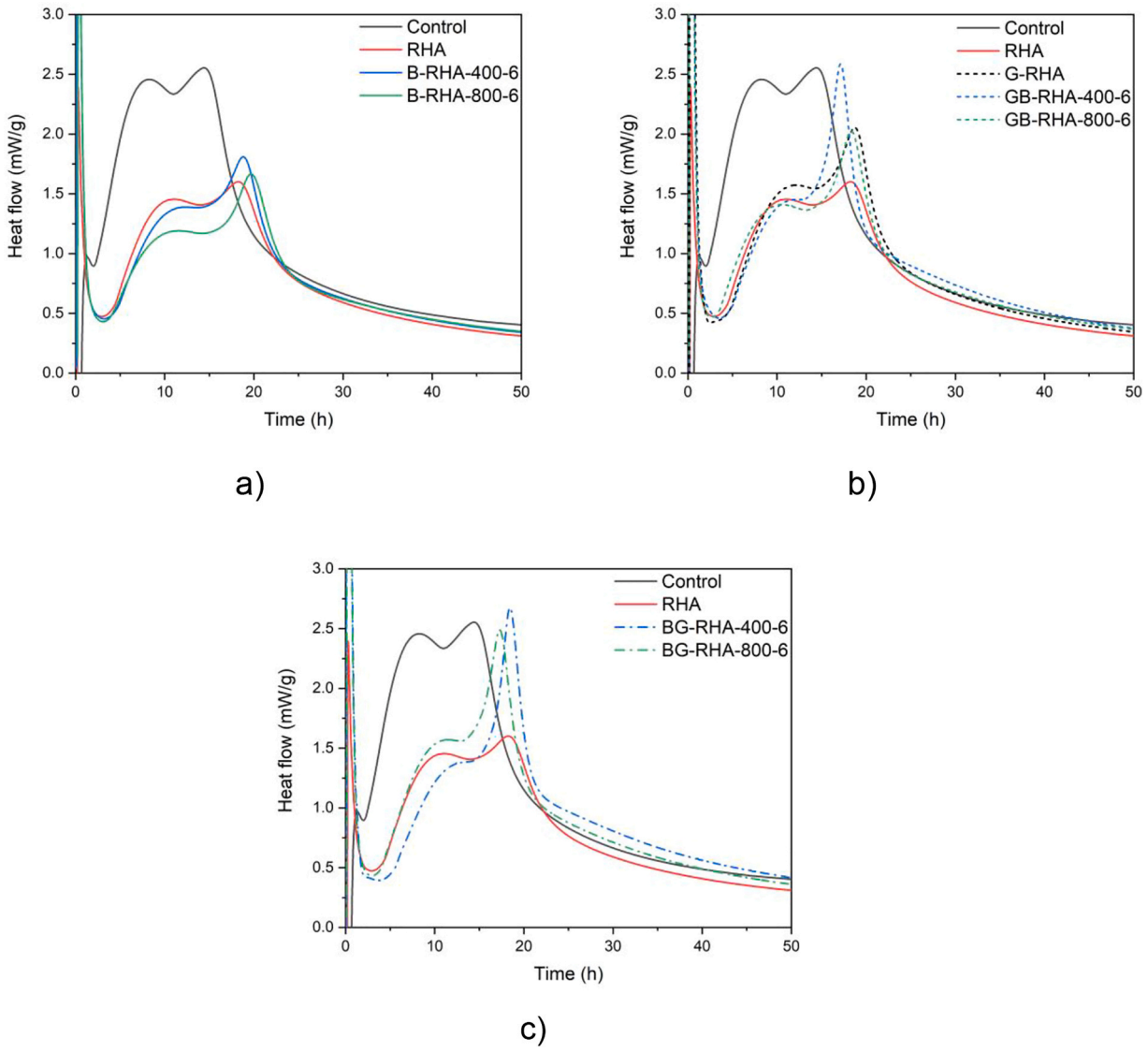

Fig. 7. Heat flow for control mortar and mortars containing raw and treated RHA, normalised by the weight of binder (milliwatt per gram of cementitious materials). a) received RHA and burnt RHA (B-RHA), b) ground RHA (G-RHA) and burnt ground RHA (GB-RHA-X-Y), c) burnt RHA followed by grinding (BG-RHA-X-Y).

Table 4).

The cumulative heat of hydration of the investigated samples rises over time (Fig. 8). The treatments positively affected the hydration kinetics. It was observed that the total cumulative heat output of the control mortar was 249.3 J/g. The replacement of 20 % wt. cement with the received RHA led to a decrease in the total cumulative heat output of the mortar to 185.5 J/g. On the other hand, thermal and grinding treatments of RHA contributed to a greater reactivity. Furthermore, burning the RHA before grinding resulted in a slightly more pronounced reactivity. The total cumulative heat output of BG-RHA-400–6 was 232.6 J/g, whilst GB-RHA-400–6 was 227.0 J/g.

3.2.2. RHA reactivity by strength index activity

To investigate the feasibility of using RHA in concrete, the strength activity index (SAI) of the ash was assessed according to [27] using cubic samples tested at 7 and 28 days of curing. SAI was calculated as follows:

$$SAI = \left(\frac{A}{B}\right) \times 100 \tag{1}$$

where A is the average compressive strength of the test pozzolan cubes (MPa) and B is the average compressive strength of the control

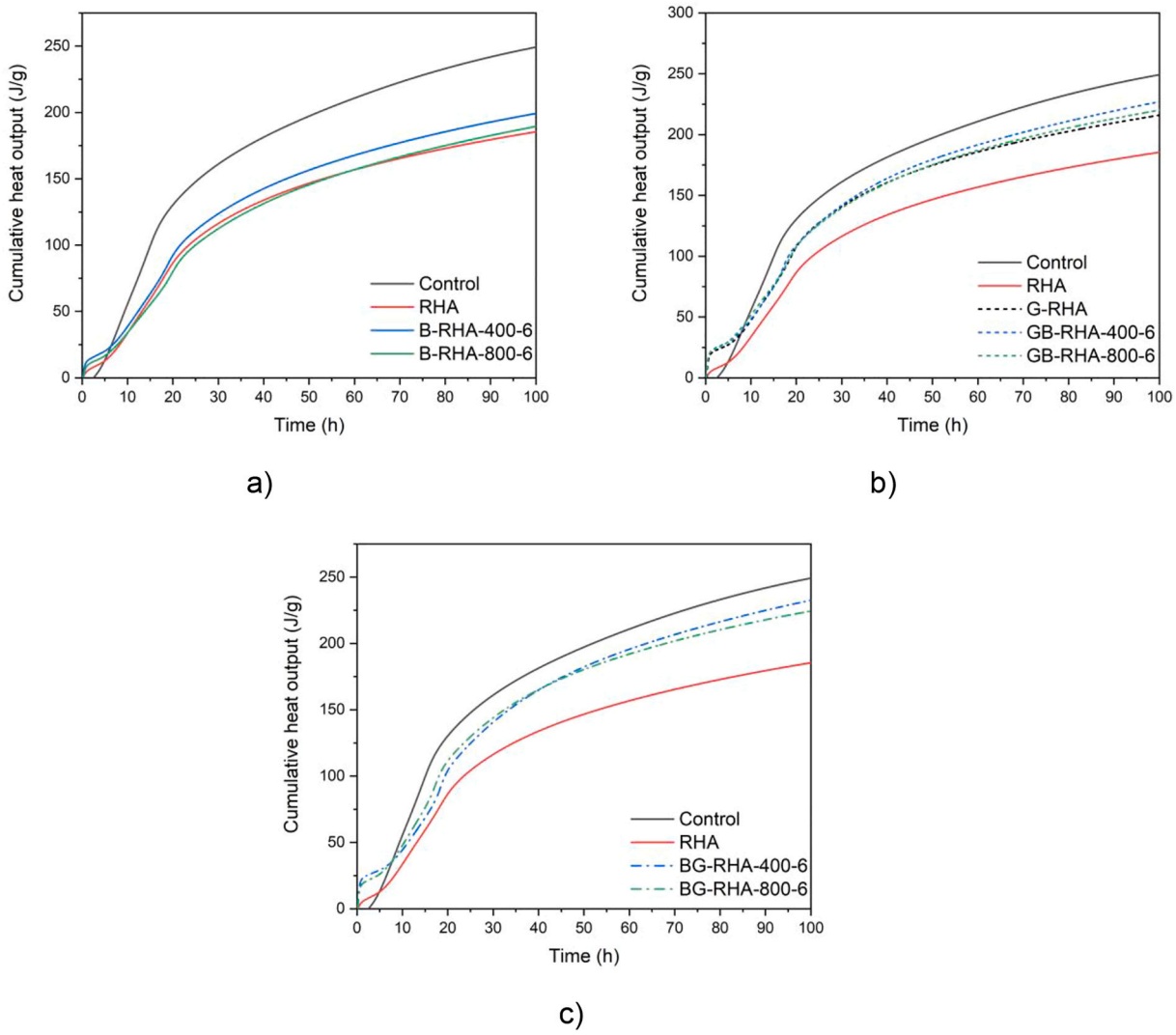

Fig. 8. Cumulative heat flow for control mortar and mortars containing raw and treated RHA (Joule per gram of cementitious materials). a) received RHA and burnt RHA (B-RHA), b) ground RHA (G-RHA) and burnt ground RHA (GB-RHA-X-Y), c) burnt RHA followed by grinding (BG-RHA-X-Y).

cubes (MPa). As per the guidelines in [39], when pozzolanic materials are substituted for Portland cement at 20 % by weight of the binder, they should result in SAI values of at least 75 % of those of the control mortar at 7 and 28 days.

The results (Fig. 9 and Fig. 10) indicate that the supplied ash (RHA) with cement in the binder does not achieve the required minimum SAI levels. Therefore, the various studied treatments were evaluated to assess whether they improved the feasibility of using the supplied RHA as a partial cement replacement in the binder.

Burning RHA can eliminate remaining carbon impurities and increase the quantity of silica in the ash [8]. Fig. 9 shows that burning temperatures up to 700 °C resulted in convergent pozzolanic activity. However, at 800 °C, the crystallinity of the silica started to be more pronounced, as previously illustrated by the XRD pattern outcomes. The burning duration also affects. For example, the B-RHA-400–6 exhibited higher pozzolanic activity than B-RHA-400–3.

However, the irregularly shaped particles (the cellular structure) of RHA associated with water adsorption (Table 2) due to the large pore size prevented the achievement of the required strength index [6]. Hence, grinding is necessary, along with heat treatment. Grinding RHA (G-RHA) to break down its cellular structure into finer particles tends to enhance RHA's pozzolanic reactivity because of the filler effects and void filling achieved, which improve the compressive strength of the mortars [17]. Decreasing the particle size of the remaining RHA increases the C-S-H content and enhances the pozzolanic activity because finer particles provide more nucleation sites [17,25]. This mitigates the adverse effect of the cellular structure of the ash particles and enhances the homogeneity of the materials.

Grinding burnt coarse RHA (BG-RHA) produces a more effective material for partial cement replacement. The cellular structure of

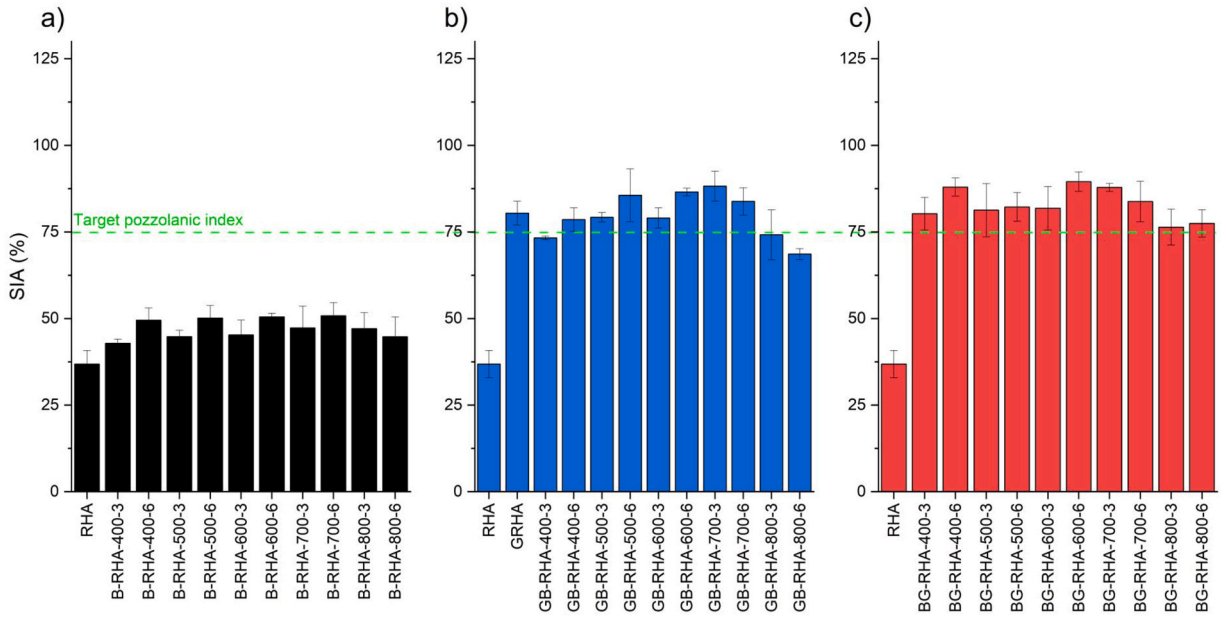

Fig. 9. The strength activity index (SAI) of the studied samples at 7-day. a) received RHA and burnt RHA (B-RHA), b) ground RHA (G-RHA) and burnt ground RHA (GB-RHA-X-Y), c) burnt RHA followed by grinding (BG-RHA-X-Y).

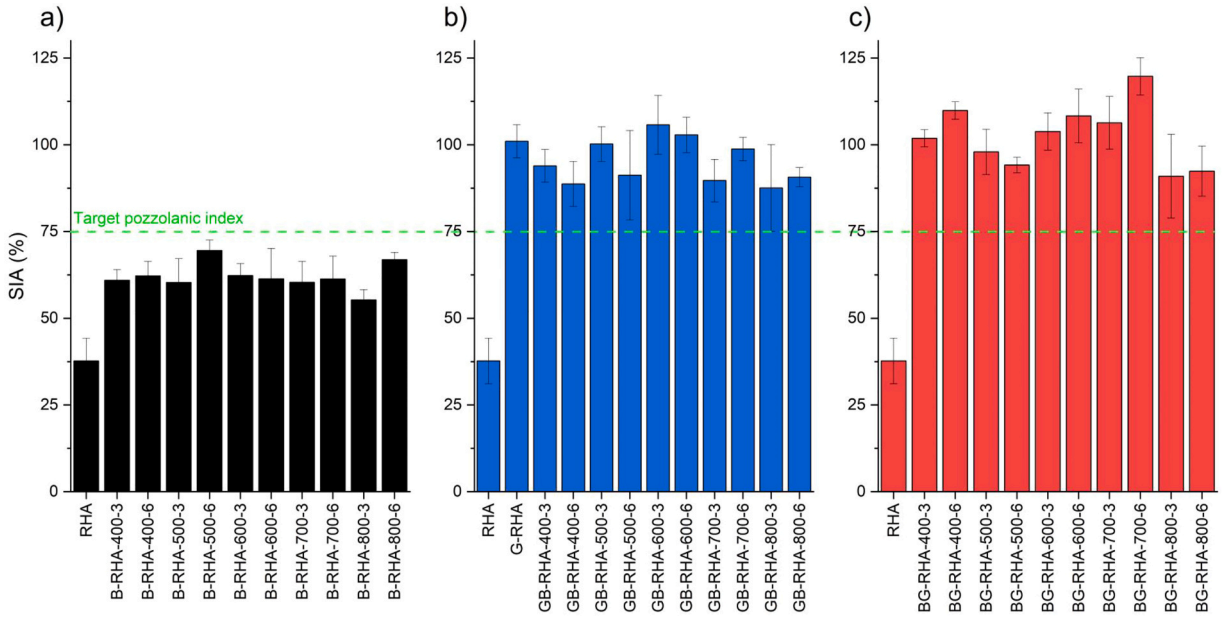

Fig. 10. The strength activity index (SAI) of the studied samples at 28-day. a) received RHA and burnt RHA (B-RHA), b) ground RHA (G-RHA) and burnt ground RHA (GB-RHA-X-Y), c) burnt RHA followed by grinding (BG-RHA-X-Y).

RHA is thought to absorb the heat of combustion in its pores, leading to more efficient combustion. Further processing of burnt RHA by grinding breaks down the cellular shape of the particles, reducing the large pore sizes responsible for water demand issues [6,40]. This ensures high-quality RHA with consistent chemical and physical properties. Grinding the RHA before burning (GB-RHA) is not the preferred sequence of treatments for producing an effective RHA cement replacement product, as illustrated in Fig. 9 and Fig. 10. Breaking the cellular structure of RHA down into finer particles is thought to make the particles more packed and agglomerated and can make it more difficult to burn the particles completely, resulting in incomplete combustion and poor pozzolanic activity.

4. Discussion on the study of RHA treatment

Table 4 shows, further thermal treatment of the received RHA resulted in variation in the amount of carbon in the ash. This variation arises from the oxidation of restricted carbon and the elimination of the K_2O layer. Prior to the removal of carbon from the ash, if the temperature reaches a level sufficient to cause surface melting of the ash, at which the K_2O layer decomposes, carbon becomes confined in the melted surface, and crystallisation of the silica is accelerated [11]. Once the carbon becomes restricted in this way, it cannot be oxidised as easily, as it becomes shielded from direct contact with the air, even at higher burning temperatures [11, 41]. When RHA particles are heated uniformly, it is possible for the remaining carbon to oxidise before the decomposition temperature of K_2O is reached [11]. Before grinding, the RHA particles tend to have a honeycomb arrangement with numerous holes (Fig. 4.c). These small holes likely contribute to significant heat absorption between particles, resulting in a more uniform temperature distribution. However, if sudden and heterogeneous heating occurs, the remaining carbon can be confined to the melt, preventing its oxidation. As a result, the LOI% of RHA particles (Table 4) subjected to grinding prior to burning is higher than that of RHA particles which are thermally treated before grinding. Breaking down the cellular structure of RHA into finer particles makes the silica in the particles more susceptible to temperature effects. As Fig. 5.a, b, and c show, RHA particles are more spherical and therefore can be packed and agglomerated. This can result in more heat stress on the exposed surfaces of the particles, resulting in a heterogeneous temperature distribution. The crystallisation point was not evident from the XRD results, but it appeared to be pronounced at 800 °C, which exceeds the surface melting temperature. This effect was more pronounced in the GB-RHA-X-Y than in the BG-RHA-X-Y. The effect of molten layers on the crystallisation of SiO_2 was apparent in the heat of hydration and pozzolanic activity, with BG-RHA-X-Y resulting in a higher peak in hydration and higher pozzolanic activity than GB-RHA-X-Y, as it delays crystallisation of the silica in RHA.

The above results indicate that burning RHA before grinding increases the temperature required to reach the melting point to decompose K_2O while burning ground RHA decreases this temperature threshold. This suggests that thermal treatment of RHA before grinding can effectively remove residual carbon in the RHA. This underscores the importance of meticulously managing the treatment procedure to prevent unfavourable reactions and successfully eliminate carbon from the RHA. A thorough understanding of the relationship between the microstructure of RHA and its responses to the thermal treatment is vital for optimising the material to meet various application requirements. Further studies are required to investigate this in more detail.

5. Conclusion

In this study, the impact of the microstructural characteristics of RHA on its responses to burning treatment was investigated to assess its effect on the pozzolanic reactivity of RHA in cement binders. The following conclusions were drawn from the results:

- The sequential treatment of burning followed by grinding produces a material with a lower LOI value and increased fineness due to more destruction of the impurities and leaving pores. The decomposition of potassium oxide (K_2O) at high temperature can result in restricts the carbon from oxidising and accelerates the crystallization, which occur earlier when grinding RHA prior burning.
- The effect of the burning RHA on its silica nature as shown by XRD patterns, was minimal. However, the crystallisation of silica phases was pronounced at 800 °C, particularly for ground RHA that was subsequently burned.
- The hydration kinetic of mortars incorporating received RHA are deteriorated due to excess residual carbon, but improvement is observed with proposed treatments. Additionally, the heat of hydration results supports the beneficial of applying a process of burning RHA followed by grinding showing its possibility to enhance the cumulative heat output and develop its pozzolanic activity in the mortar.
- The findings underscore the importance of rigorously managing the thermal treatment and grinding of RHA to enhance its effectiveness as supplementary cementitious material. Properly managing sequence treatment between burning and grinding is vital step in developing a product with the desired properties for use as a partial replacement for cement in concrete applications.

Further research is needed to investigate the scalability of the proposed treatment to enhance the application of residual RHA in the binder. This will assess to solidify the role of RHA as effective cement replacement.

CRediT authorship contribution statement

Ayman Almutlaqah: Writing – original draft, Investigation, Formal analysis, Data curation, Conceptualization. **Sivakumar Kulasegaram:** Writing – review & editing, Supervision, Project administration. **Riccardo Maddalena:** Writing – review & editing, Supervision, Methodology.

Declaration of Competing Interest

The authors declare that they have no known competing financial interests or personal relationships that could have appeared to influence the work reported in this paper.

Data availability

Data will be made available on request.

References

[1] H. Asadi, M. Ghorbani, M. Rezaei-Rashti, S. Abrishamkesh, E. Amirahmadi, C. Chengrong, M. Gorji, Application of rice husk biochar for achieving sustainable agriculture and environment, Rice Sci. 28 (2021) 325–343, https://doi.org/10.1016/J.RSCI.2021.05.004.

[2] H.T. Le, H.M. Ludwig, Effect of rice husk ash and other mineral admixtures on properties of self-compacting high performance concrete, Mater. Des. 89 (2016) 156–166, https://doi.org/10.1016/j.matdes.2015.09.120.

[3] J. Payá, J. Monzó, M.V. Borrachero, E. Peris-Mora, L.M. Ordóñez, Studies on crystalline rice husk ashes and the activation of their pozzolanic properties, in: Waste Management Series, Elsevier, 2000, pp. 493–503, https://doi.org/10.1016/S0713-2743(00)80060-4.

[4] R.K. Sandhu, R. Siddique, Influence of rice husk ash (RHA) on the properties of self-compacting concrete: a review, Constr. Build. Mater. 153 (2017) 751–764, https://doi.org/10.1016/j.conbuildmat.2017.07.165.

[5] WAP, Rice Production by Country - World Agricultural Production 2020/2021, (2021). ⟨http://www.worldagriculturalproduction.com/crops/rice.aspx⟩.

[6] V. Jittin, A. Bahurudeen, S.D. Ajinkya, Utilisation of rice husk ash for cleaner production of different construction products, J. Clean. Prod. 263 (2020) 121578, https://doi.org/10.1016/j.jclepro.2020.121578.

[7] S. Kumar, A. Adediran, C. Rodrigue, S. Mohammed, N. Leklou, Production, characteristics, and utilization of rice husk ash in alkali activated materials: an overview of fresh and hardened state properties, Constr. Build. Mater. 345 (2022) 128341, https://doi.org/10.1016/j.conbuildmat.2022.128341.

[8] V.P. Della, I. Kühn, D. Hotza, Rice husk ash as an alternate source for active silica production, Mater. Lett. 57 (2002) 818–821, https://doi.org/10.1016/S0167-577X(02)00879-0.

[9] R. Zerbino, G. Giaccio, G.C. Isaia, Concrete incorporating rice-husk ash without processing, Constr. Build. Mater. 25 (2011) 371–378, https://doi.org/10.1016/j.conbuildmat.2010.06.016.

[10] A. Siddika, M.A.Al Mamun, R. Alyousef, H. Mohammadhosseini, State-of-the-art-review on rice husk ash: a supplementary cementitious material in concrete, J. King Saud. Univ. - Eng. Sci. 33 (2021) 294–307, https://doi.org/10.1016/j.jksues.2020.10.006.

[11] R.V. Krishnarao, J. Subrahmanyam, T.Jagadish Kumar, Studies on the formation of black particles in rice husk silica ash, J. Eur. Ceram. Soc. 21 (2001) 99–104, https://doi.org/10.1016/S0955-2219(00)00170-9.

[12] V. Kannan, Strength and durability performance of self compacting concrete containing self-combusted rice husk ash and metakaolin, Constr. Build. Mater. 160 (2018) 169–179, https://doi.org/10.1016/j.conbuildmat.2017.11.043.

[13] S. Muthukrishnan, S. Gupta, H.W. Kua, Application of rice husk biochar and thermally treated low silica rice husk ash to improve physical properties of cement mortar, Theor. Appl. Fract. Mech. 104 (2019) 102376, https://doi.org/10.1016/j.tafmec.2019.102376.

[14] K. Ganesan, K. Rajagopal, K. Thangavel, Rice husk ash blended cement: assessment of optimal level of replacement for strength and permeability properties of concrete, Constr. Build. Mater. 22 (2008) 1675–1683, https://doi.org/10.1016/j.conbuildmat.2007.06.011.

[15] W. Xu, J. Wei, J. Chen, B. Zhang, P. Xu, J. Ren, Q. Yu, Comparative study of water-leaching and acid-leaching pretreatment on the thermal stability and reactivity of biomass silica for viability as a pozzolanic additive in cement, Materials 11 (2018), https://doi.org/10.3390/ma11091697.

[16] S. Rukzon, P. Chindaprasirt, R. Mahachai, Effect of grinding on chemical and physical properties of rice husk ash, Int. J. Miner., Metall. Mater. 16 (2009) 242–247, https://doi.org/10.1016/S1674-4799(09)60041-8.

[17] H. Chao-Lung, B.Le Anh-Tuan, C. Chun-Tsun, Effect of rice husk ash on the strength and durability characteristics of concrete, Constr. Build. Mater. 25 (2011) 3768–3772, https://doi.org/10.1016/j.conbuildmat.2011.04.009.

[18] D.M. Ibrahim, M. Helmy, Crystallite growth of rice husk ash silica, Thermochim. Acta 45 (1981) 79–85, https://doi.org/10.1016/0040-6031(81)80057-3.

[19] S. Hanafi, S.A. Abo-El-Enein, D.M. Ibrahim, S.A. El-Hemaly, Surface properties of silicas produced by thermal treatment of rice-husk ash, Thermochim. Acta 37 (1980) 137–143, https://doi.org/10.1016/0040-6031(80)80034-7.

[20] L. Xiong, E.H. Sekiya, S. Wada, K. Saito, Burning temperature dependence of rice husk ashes in structure and property, ACS Appl. Mater. Interfaces 19 (2009) 95–99.

[21] Q. Yu, K. Sawayama, S. Sugita, M. Shoya, Y. Isojima, The reaction between rice husk ash and Ca(OH)2 solution and the nature of its product, Cem. Concr. Res 29 (1999) 37–43, https://doi.org/10.1016/S0008-8846(98)00172-0.

[22] D.G. Nair, A. Fraaij, A.A.K. Klaassen, A.P.M. Kentgens, A structural investigation relating to the pozzolanic activity of rice husk ashes, Cem. Concr. Res 38 (2008) 861–869, https://doi.org/10.1016/j.cemconres.2007.10.004.

[23] M. Sarangi, P. Nayak, T.N. Tiwari, Effect of temperature on nano-crystalline silica and carbon composites obtained from rice-husk ash, Compos B Eng. 42 (2011) 1994–1998, https://doi.org/10.1016/j.compositesb.2011.05.026.

[24] P.K. Metha, Siliceous ashes and hydraulic cements prepared therefrom., U.S.4,105,459, 1978.

[25] W. Xu, Y.T. Lo, D. Ouyang, S.A. Memon, F. Xing, W. Wang, X. Yuan, Effect of rice husk ash fineness on porosity and hydration reaction of blended cement paste, Constr. Build. Mater. 89 (2015) 90–101, https://doi.org/10.1016/j.conbuildmat.2015.04.030.

[26] EN 197-1, Cement - Part 1: Composition, specifications and conformity criteria for common cements Ciment, EUROPEAN COMMITTEE FOR STANDARDIZATION (2019).

[27] ASTM C 311, Standard test methods for sampling and testing fly ash or natural pozzolans for use in Portland-cement concrete, ASTM Stand. 04 (02) (2022) 204–212, https://doi.org/10.1520/C0311_C0311M-22.

[28] ASTM D734, Standard test methods for loss on ignition (LOI) of solid combustion residues annual book of ASTM, standards, ASTM Stand. 04 (2021) 1–7, https://doi.org/10.1520/D7348-21.

[29] calmetrix, I-Cal 8000 HPC _ calmetrix, (2023). ⟨https://www.calmetrix.com/i-cal-8000-hpc⟩.

[30] A.P. Vieira, R.D. Toledo Filho, L.M. Tavares, G.C. Cordeiro, Effect of particle size, porous structure and content of rice husk ash on the hydration process and compressive strength evolution of concrete, Constr. Build. Mater. 236 (2020) 117553, https://doi.org/10.1016/j.conbuildmat.2019.117553.

[31] M. Sarangi, S. Bhattacharyya, R.C. Behera, Effect of temperature on morphology and phase transformations of nano-crystalline silica obtained from rice husk, Phase Transit. 82 (2009) 377–386, https://doi.org/10.1080/01411590902978502.

[32] A. Muthadhi, S. Kothandaraman, Optimum production conditions for reactive rice husk ash, Mater. Struct. /Mater. Et. Constr. 43 (2010) 1303–1315, https://doi.org/10.1617/s11527-010-9581-0.

[33] N. Van Tuan, G. Ye, K. Van Breugel, O. Copuroglu, Hydration and microstructure of ultra high performance concrete incorporating rice husk ash, Cem. Concr. Res 41 (2011) 1104–1111, https://doi.org/10.1016/j.cemconres.2011.06.009.

[34] X. Luo, X. Jiang, Q. Chen, Z. Huang, An assessment method of hydration degree of Rice husk ash blended cement considering temperature effect, Constr. Build. Mater. 304 (2021) 124534, https://doi.org/10.1016/j.conbuildmat.2021.124534.

[35] J. Wang, J. Xiao, Z. Zhang, K. Han, X. Hu, F. Jiang, Action mechanism of rice husk ash and the effect on main performances of cement-based materials: a review, Constr. Build. Mater. 288 (2021) 123068, https://doi.org/10.1016/j.conbuildmat.2021.123068.

[36] J. Beaudoin, I. Odler. Hydration, Setting and Hardening of Portland Cement, 5th ed., Elsevier Ltd, 2019 https://doi.org/10.1016/B978-0-08-100773-0.00005-8.

[37] J.W. Bullard, H.M. Jennings, R.A. Livingston, A. Nonat, G.W. Scherer, J.S. Schweitzer, K.L. Scrivener, J.J. Thomas, Mechanisms of cement hydration, Cem. Concr. Res 41 (2011) 1208–1223, https://doi.org/10.1016/j.cemconres.2010.09.011.

[38] R. Maddalena, C. Hall, A. Hamilton, Effect of silica particle size on the formation of calcium silicate hydrate [C-S-H] using thermal analysis, Thermochim. Acta 672 (2019) 142–149, https://doi.org/10.1016/j.tca.2018.09.003.

[39] ASTM C618, Standard specification for coal fly ash and raw or calcined natural pozzolan for use, ASTM Stand. (2022) 3–6, https://doi.org/10.1520/C0618-22.

[40] L. Prasittisopin, D. Trejo, Hydration and phase formation of blended cementitious systems incorporating chemically transformed rice husk ash, Cem. Concr. Compos 59 (2015) 100–106, https://doi.org/10.1016/j.cemconcomp.2015.03.002.

[41] J. Shen, X. Liu, S. Zhu, H. Zhang, J. Tan, Effects of calcination parameters on the silica phase of original and leached rice husk ash, Mater. Lett. 65 (2011) 1179–1183, https://doi.org/10.1016/j.matlet.2011.01.034.